Arxiv: 2311.18731

JADES: A large population of obscured, narrow line AGN at high redshift

Jan Scholtz[1,2,*], Roberto Maiolino[1,2,3], Francesco D'Eugenio[1,2] Emma Curtis-Lake[4], Stefano Carniani[5], Stephane Charlot[6], Mirko Curti[7], Maddie S. Silcock[4], Santiago Arribas[8], William Baker[1,2], Rachana Bhatawdekar[9], Kristan Boyett[10,11], Andrew J. Bunker[12], Jacopo Chevallard[12], Chiara Circosta[9], Daniel J. Eisenstein[13], Kevin Hainline[14], Ryan Hausen[15], Xihan Ji[1,2], Zhiyuan Ji[14], Benjamin D. Johnson[13], Nimisha Kumari[16], Tobias J. Looser[1,2], Jianwei Lyu[14], Michael V. Maseda[17], Eleonora Parlanti[5], Michele Perna[9], Marcia Rieke[14], Brant Robertson[18], Bruno Rodríguez Del Pino[9], Fengwu Sun[14], Sandro Tacchella[1,2], Hannah Übler[1,2], Giacomo Venturi[5], Christina C. Williams[19], Christopher N. A. Willmer[14], Chris Willott[20], and Joris Witstok[1,2]

ABSTRACT

We present the identification of 42 narrow-line active galactic nuclei (type-2 AGN) candidates in the two deepest observations of the JADES spectroscopic survey with JWST/NIRSpec. The spectral coverage and the depth of our observations allow us to select narrow-line AGNs based on both rest-frame optical and UV emission lines up to z=10. Due to the metallicity decrease of galaxies, at z > 3 the standard optical diagnostic diagrams (N2-BPT or S2-VO87) become unable to distinguish many AGN from other sources of photoionisation. Therefore, we also use high ionisation lines, such as He II λ4686, He II λ1640, [Ne IV] λ2422, [Ne V] λ3420, and N V λ1240, also in combination with other UV transitions, to trace the presence of AGN. Out of a parent sample of 209 galaxies, we identify 42 type-2 AGN (although 10 of them are tentative), giving a fraction of galaxies in JADES hosting type-2 AGN of about 20 ± 3%, which does not evolve significantly in the redshift range between 2 and 10. The selected type-2 AGN have estimated bolometric luminosities of $10^{41.3-44.9}$ erg s^{-1} and host-galaxy stellar masses of $10^{7.2-9.3}$ M$_\odot$. The star formation rates of the selected AGN host galaxies are consistent with those of the star-forming main sequence. The AGN host galaxies at z=4-6 contribute ~8-30 % to the UV luminosity function, slightly increasing with UV luminosity.

1. Introduction:

AGNs (SMBHs) have a tight correlation to the host galaxies bulge properties. Also the feedback from AGNs can greatly affect galaxy evolution by changing the ISM.

Identifying AGNs at **high-z** can help us understand not only the co-evolution of SMBHs and galaxies, but also the formation of galaxies at early epochs.

Before JWST: limited to bright quasars, including the most distant quasars at z ~ 7.5

Earlier JWST results: a. identified by performing SEDs of broad-band photometry (Furtak+22; Onoue+23…); **b.** the presence of a broad line region (BLR; Furtak+23, Harikane+23…)

→ AGN at z=4-11, with estimated black hole masses (M_{BH}) in the range 10^6 to 10^8 $M_\odot$ and bolometric luminosities $10^{44} - 10^{45}$ $erg\ s^{-1}$.

Identification of narrow-line (type-2) AGNs remained unexplored.

The low metallicity and high ionization parameter at z > 3 make the classical emission-line diagnostic diagrams (such as BPT) less successful.

Photo-ionization grid models show the nebular emission of star-forming galaxies at high-z become similar to that of AGN.

The identification of type-2 AGN at high redshift can still rely on high ionization lines, such as the [Ne iv] λ2424 (with ionization potential >63.45eV; Brinchmann 2023).

2. Observations, Data reduction and Analysis:

JADES survey by JWST/NIRSpec MSA with 5(3) filter combinitions in two programms

Both have very long exposures > 10hrs.

GTO Data Reduction pipeline in Carniani et al. (in prep), summarized in Bunker+23a.

Spectral fitting using **PPXF**: SSP spectra from FSPS to fit continuum; Single Gaussian functions to fit the emission lines.

The stellar kinematics are tied to Balmer iine kinematcis. Excepting PRISM data, multiplets (e.g., $C_{IV}\lambda\lambda$1548,1551, $C_{III}]\lambda\lambda$1907,1909, [O II] doublets, [S II] doublets) are fitted with varaible ratios.

High ionization UV lines ([Ne_{IV}]λ2424, [Ne_V]λ3426, N_V λ1240) were excluded from the pPXF fitting as they are extremely faint. Only fitting objects with [O III] or Hα SNR >10 by **QubeSpec.** (Only 7 objects detected with these lines)

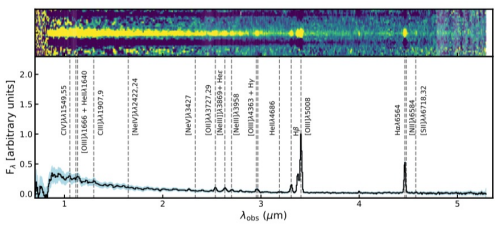

Fig. 1: Example of low-resolution PRISM/CLEAR spectrum of galaxy (JADES-NS-GS-00022251) at z = 5.804 included in our parent sample. The spectrum is shown in units of F_λ normalized to the [O III] λ5008 peak. We highlight major emission lines used in our analysis.

SED fitting using BEAGLE: SFRs of from BEAGLE are in excellent agreement with those estimated from the dust-corrected Balmer lines.

Comparison to photoioinization models in Feltre et al. (2016), Gutkin et al. (2016) and Nakajima & Maiolino (2022).

Diagnostics	Line Ratio
R3	[O III]λ5008 / Hβ
N2	[N II]λ6584 / Hα
S2	[S II]λλ6718,32 / Hα
Ne3O2	[Ne III]λ3869 / [O II]λλ3727,29
He2	He IIλ4686 / Hβ
C43	C IVλλ1549,51/C IIIλλ1906,08
C3He2	C IIIλλ1906,08 / He IIλ1640
Ne4C3	[Ne IV] λλ2422,24/C IIIλλ1906,08
Ne5C3	[Ne V] λλ3427,29/C IIIλλ1906,08
N5C3	N V λλ1239,42/C IIIλλ1906,08

Emission line	λ_{rest}(Å)	Ionisation potential (eV)
[S II]	6718,32	10.7
[N II]	6584,48	14.5
Hα	6563	13.6
[O III]	5008,4961	35.1
Hβ	4861	13.6
He II	4686	54.4
[O II]	3727,29	13.6
[Ne III]	3689	41.0
[Ne V]	3427	97.11
[Ne IV]	2422,24	77.2
C III]	1907,09	24.4
He II	1640	54.4
C IV	1548,1550	47.9
[N V]	1239,42	77

3. Selection of AGN in JADES deep spectroscopic data

Requting 3σ detection of the following lines: Hα, Hβ, [O_{III}] and [C_{III}]

Wavelength coverages of optical and UV line selection

→ 209 sources

Selecting AGN based on various emission lines

A. N2–R3 and S2–R3 planes (also known as BPT and VO87

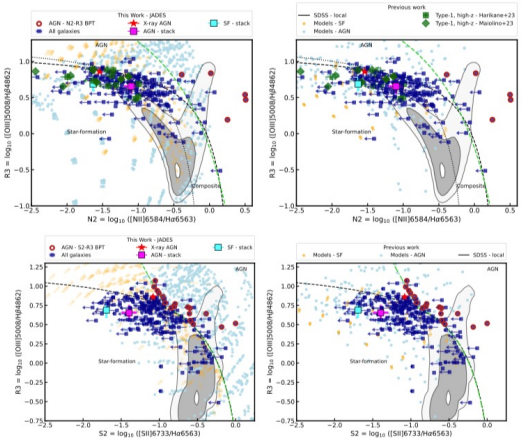

Fig. 2: Typical line ratio diagnostic diagrams used to select AGN. N2-R3 BPT ([N II]/Hα vs [O III]/Hβ; top row) and S2-VO87 ([S II]/Hα vs [O III]/Hβ; bottom row). The ionisation models of Feltre et al. (2016); Gutkin et al. (2016) (left) and Nakajima & Maiolino (2022) (right) are reported as yellow (SF) and blue (AGN) points (see §2.4). The objects from this work are plotted as blue squares. The objects selected as AGN based in these diagrams are highlighted by red circles. We also plot our new demarcation lines as green dashed. The black dashed lines show the star forming versus AGN demarcation lines from Kewley et al. (2001) and Kauffmann et al. (2003). For comparison, we plot SDSS galaxies shown as a grey contour plot. The magenta and cyan squares show a stacked spectrum for AGN and star-forming galaxies (see §4.1). We highlight type-1 AGN from Harikane et al. (2023) and Maiolino et al. (2023a) as green squares and diamonds. The red star shows the X-ray selected AGN in our sample.

Lower metallicity leads to fainter [N_{II}] lines & Higher ionization parameters gives higher R3. → Shifting AGN towards the locus of star forming galaxies, makes AGN and SF galaxies largely overlap at high-z.

From the photo-ionization models, we also see that SF galaxies can lie in the AGN part of the BPT diagram at high redshift with R3 > 0.9.

A conservative way to classify AGN: define the edge of the star-forming region using the points with the highest [N_{II}]/Hα values from photo-ionization model (green dashed line).

N2-BPT: $R3 = \frac{3.09}{(N2-1.03)} + 2.78$ (only 5 candidates, red circles)

S2-BPT: $R3 = \frac{0.78}{(S2-0.34)} + 1.36$; $R3 = -0.91 - 1.79 * S2$ $(S2 < -0.92)$

(17 candidates but several located at the edge)

B. HeII λ4686 emission line, He2-N2 diagram (Shirazi & Brinchmann+12)

HeII is nearly independent of the metallicity and ionization parameter, depending instead primarily on the shape of the ionizing spectrum, more specifically on the number of ionizing photons > 54 eV.

9 sources have detection of HeII λ4686, all above the black dashed line + 3 sources have N2 > 0.2 → select 12 AGN in total from this figure.

(still showing complexity of selecting AGN at high redshift because of a lots of upper limit)

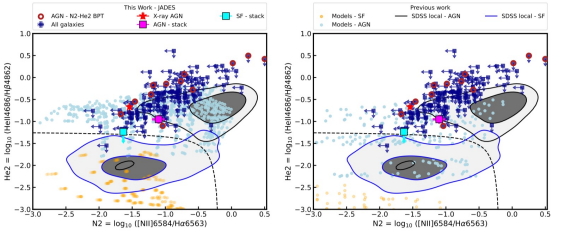

Fig. 3: The He2-N2 (He II/Hβ vs [N II]/Hα) diagram for the sample of JADES galaxies for our sample, plotted as blue squares. The left and right plots show ionisation models from Feltre et al. (2016); Gutkin et al. (2016) and Nakajima & Maiolino (2022), respectively, as yellow and light blue points (see §2.4). The magenta and cyan squares show a stacked spectrum for AGN and star-forming galaxies (see §4.1). The black dashed line indicates a demarcation line between star-forming and AGN galaxies by Shirazi & Brinchmann (2012). The blue and black contours show the star-forming galaxies and AGN from SDSS, respectively. We highlight the selected AGN in this diagram with a red circle.

C. UV line diagnostics

High-ionization lines, including [Ne_{IV}]λ2424, [Ne_V]λ3426, N_V λ1240 require high energy photons, that can hardly be produced by star-formation processes. The authors identified 6 sources may be AGNs. Past works have suggested brighter UV emission lines ratios based on $C_{III}]\lambda\lambda$1907,09, $C_{IV}\lambda\lambda$1548,51, [O_{III}]λλ1660,66 and He_{II} λ1640.

1 source in AGN, 4 sources in composite regions

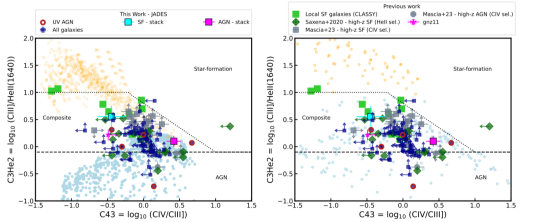

Fig. 4: C III]/He II λ1640 vs C IV/C III](CHe2-C43) diagnostic diagram. We plot our sample as blue squares. The left and right plots show ionisation models from Feltre et al. (2016); Gutkin et al. (2016) and Nakajima & Maiolino (2022), respectively, as yellow and light blue points (see §2.4). The green diamonds show He II λ1640 detection from the VANDELS survey (Saxena et al. 2020), and all C IV detections from Mascia et al. (2023) as grey colour with squares and circles representing SF and AGN, respectively. The green squares show local analogues of high-redshift galaxies (from CLASSY survey; Mingozzi et al. 2023). We also show the black dashed and dotted demarcation lines between AGN, star-forming galaxies and composite line ratios from Hirschmann et al. (2022). Overall, we select five AGN on this diagram and we highlight these with a red circle. The magenta and cyan squares show a stacked spectrum for AGN and star-forming galaxies (see §4.1).

 # The UV emission line diagnostic requires the detection of three UV emission lines. Despite the excellent sensitivity of JWST/NIRSpec, detecting all three UV emission lines is still a challenge for exposures <10 hours.

→ 42 AGN candidates, from at least one of the different selection methods investigated in Section 3 in the redshift range of 1.4–9.4.

4. Discussion

A. Stacking spectrum properties:

AGN at high-z are [NII] weak and have a [OIII]/Hβ ratio very similar to star-forming galaxies.

HeII λ4686/Hβ vs [NII]/Hα diagram shows a separation of SF and AGN galaxies. (Ideal tracer)

Much stronger CIV indicated much higher and harder ionization field in AGN host galaxies.

Sample	AGN Optical	AGN UV	SF Optical	SF UV
N	20	9	55	31
z_{median}	3.87	5.93	4.77	5.91
Fluxes	(×10^{-20}	erg s^{-1} cm^{-2})		
Hα	$114.5^{+1.7}_{-1.6}$	-	$66.5^{+0.8}_{-0.8}$	-
[N II]	$16.6^{+1.0}_{-1.0}$	-	$2.5^{+0.4}_{-0.4}$	-
[S II]	$4.5^{+2.0}_{-1.7}$	-	$1.6^{+0.5}_{-0.5}$	-
[O III]	$222.2^{+1.9}_{-2.0}$	-	$113.3^{+0.8}_{-0.8}$	-
Hβ	$48.8^{+1.5}_{-1.5}$	-	$24.1^{+0.6}_{-0.7}$	-
He II λ4686	$6.6^{+1.5}_{-1.1}$	-	< 10.5	-
C III]	-	$20.7^{+3.8}_{-3.7}$	-	$16.5^{+1.9}_{-1.8}$
C IV	-	$59.0^{+4.6}_{-4.6}$	-	$6.1^{+1.7}_{-1.5}$
He II λ1640	-	$18.6^{+3.3}_{-3.3}$	-	$4.2^{+1.3}_{-1.3}$

HeII traces a hard ionising radiation, with which AGN activity is the most likely source. However, other sources can also produce HeII emission such as Wolf-Rayet stars, X-ray binaries, and some more exotic star-formation processes.

B. AGN luminosities

The bolometric luminosities (L_{bol}) are derived from the narrow line fluxes of Hβ , [OIII] and C_{III}]

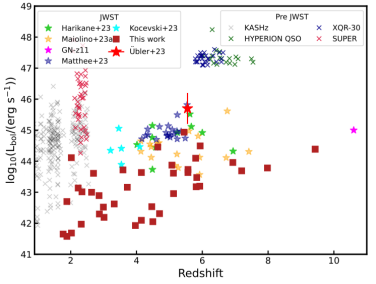

This work are now probing, AGN at z>3 that are 2-3 orders of magnitude less luminous than previous surveys, understanding the broader demographics of the AGN population in the early Universe.

C. Contribution of AGN host galaxies to the UV luminosity function

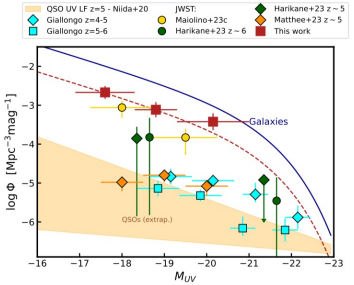

Estimating the contribution of AGN host galaxies to the UV luminosity function simply as the fraction of AGN identified in UV luminosity bins. (33 %, 18 % and 20 %, for the M_{UV} = -20.15, -18.8, -17.6 bins)

Type 2 AGN host galaxies contribute to ~20% to the reionization of the Universe.